Chapter 8
Quasi-Real Time Determination of 2013 Lushan Mw 6.6 Earthquake Epicenter, Trigger Time and Magnitude Using 50 Hz GPS Observations

Meng Li, Dingfa Huang, Li Yan, Weifeng Chen, Hua Liao, Tie Gu and Na Chen

Abstract 50 HZ Global Positioning System (GPS) high rates data of 8 Continual Operation Reference System (CORS) sites nearby Lushan are used to analyze the earthquake trigger time, epicenter and magnitude. All sites position time series on N, E directions are resolved with the track software, and horizontal accuracy can reach to 2 cm at least. Horizontal position time series analyses show that the earthquake mainly affects QLAI, SCTQ, YAAN sites, the horizontal peak amplitudes can reach to 50 mm, the maximum instantaneous velocity can reach to 72.36 mm/s and the maximum instantaneous acceleration have reached to 105.9 mm/s^2. Analyzing the position time series by the method of S transformation, the arrival time of seismic wave is estimated. With seismic wave arriving time and coordinates of three sites which are first detecting the seismic wave, the earthquake's epicenter and trigger time can be fast determined by three-dimensional search method. Moreover, the earthquake magnitude can also be estimated by horizontal peak amplitudes from the sites using the regression method. These suggest exiting GPS infrastructure could be developed into an effective component of earthquake assessment.

Keywords Lushan Earthquake · CORS · High rate GPS · Epicenter · Magnitude

M. Li · D. Huang (✉) · L. Yan · N. Chen
Faculty of Geosciences and Environment Engineering, Southwest Jiaotong University,
Chengdu 610031, China
e-mail: dfhuang@home.swjtu.edu.cn

M. Li
e-mail: nemon818@163.com

W. Chen · H. Liao · T. Gu
Disaster Relief Research Institute, Sichuan Seismological Bureau,
Chengdu 610041, China

8.1 Introduction

The 20 April 2013 Lushan earthquake with the magnitude of Mw 6.6 occurred on the southern segment of the Longmen Shan fault in Sichuan, China. Nearly 200 persons were killed and the economic loss was reached to 170 billion yuan. Once a destructive seismic event occurs, the magnitude determination, the nucleation location, and the seismic event trigger time will be essential for earthquake relief. However, to estimate a reliable and rapid measurement of the magnitude of an earthquake is a challenge, especially for earthquake magnitude is above 8.0 ($M > 8$) [6].

As the technique High-rate GPS whereby positions are estimated at a rate of once per second or higher using the high-precision phase observations of the GPS. In addition, comparing to seismometers, GPS has the unprecedented advantage on estimating the position time series without titling, saturation. Using GPS on seismology has become a new subject, GPS seismology [5]. This new subject springs up at the beginning of the 21th century, Developed only in the last few 5 years, and this technique has been widely used to determine the time-dependent surface displacements induced by the 2008 Wenchuan earthquake in Sichuan of China [9, 12], the 2010 Mw 8.8 Maule Megathrust Earthquake of Central Chile [4], and the 2010 Mw 7.2 El Mayor-Cucapah earthquake [2, 13]. Many researchers have pointed out the need for 10-sps GPS (or even higher sampling rate) data in seismology studies. Several 10-sps GPS seismograms from the 2009 earthquake in L'Aquila, Italy (Mw 6.3) have been used to study strong ground motions and earthquake source mechanisms [1].

Since the CORS' sites of Sichuan, China have integrity and precisely recorded the data through Lushan earthquake occurred, we mainly investigate the potential usage of high rates GPS in earthquake relief by this case in our study.

8.2 Data Processing and Horizontal Movement Characteristics

The raw observation data from Crustal Movement Observation Network of China and Seismological Bureau of Sichuan Province have recorded the detailed ground motion through Lushan Earthquake. All the receivers of CORS sites are Trimble Net8 and the receiver antennas are TRM59800. The geographical location of the CORS sites have been shown as Fig. 8.1.

Epoch-to-epoch processing of the very high rate GPS data (VHRGPS) has been described to analyze the quasi real time displacements of CORS stations in Sichuan during the Lushan earthquake. We use the teqc software provided by UNAVCO (http://www.unavco.org/) and the runpkr00 software provided by Trimble company covert the 50 Hz Trimble T02 data to rinex data, and then the high sampling rate data (50 Hz) were processed using the TRACK software of
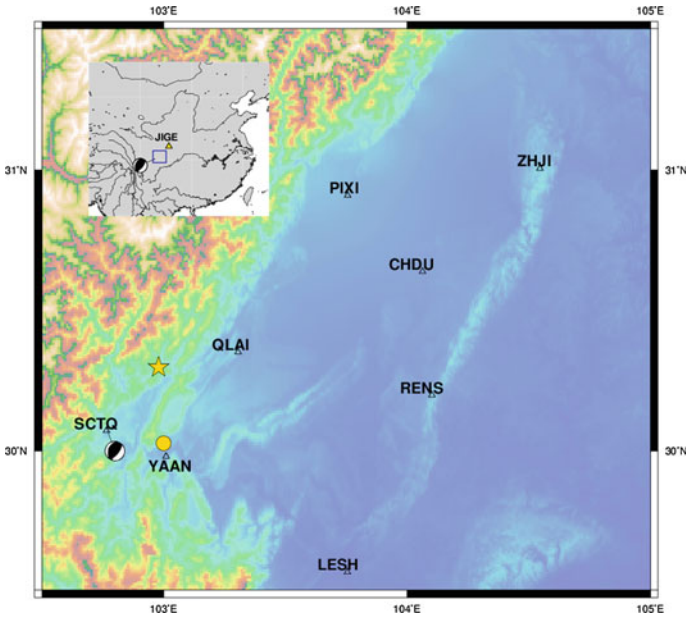
Fig. 8.1 Location of the CORS sites (Beach ball represents focal mechanism was provided by USGS, *yellow Five-pointed star* was the epicenter location provided by Chinese Seismological Bureau, *yellow circle* was the epicenter calculated in this paper, JIGE is the reference station)

GAMIT developed at MIT. The LC combination and IGS precise orbits, and apply a smoothing filter on the backward solution to estimate the atmospheric delays using the whole 24 h data and fix any non-integer biases to a constant value. Because TRACK computes a relative position with respect to a fixed reference station, we choose to use the same for all moving sites.

Since the site JIGE of our CORS network is far enough from the epicenter, the surface wave which shake this station arrives late enough so that the first 200 s are unaffected by this motion, we picked it as the base station. The JIGE site is calculated for check the motion of PENX whether the site has been affected by Lushan Earthquake. In general, it is difficult to assess the accuracy of HRGPS. Some low frequency biases related to atmosphere drift or satellite configuration changes may show, depending on the length of the baseline to the reference station. This does not affect the co-seismic step since it is an almost instantaneous displacement, but renders difficult the chase for pre-seismic or rapid post-seismic signal.

The linear terms of CORS sites deformations have been treated as useless noise and therefore removed. Velocity, acceleration of CORS sites motion have been calculated by signal and double differential of the position time series, respectively. The detailed horizontal displacement, velocity and acceleration time series have been shown by Figs. 8.2, 8.3 and 8.4. Since the accuracies of vertical position time
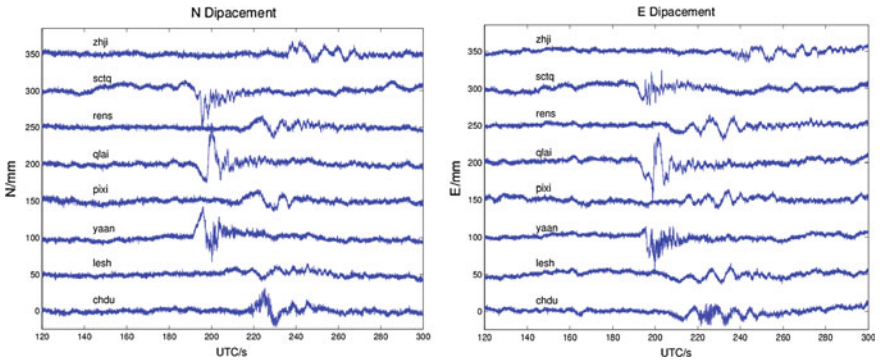
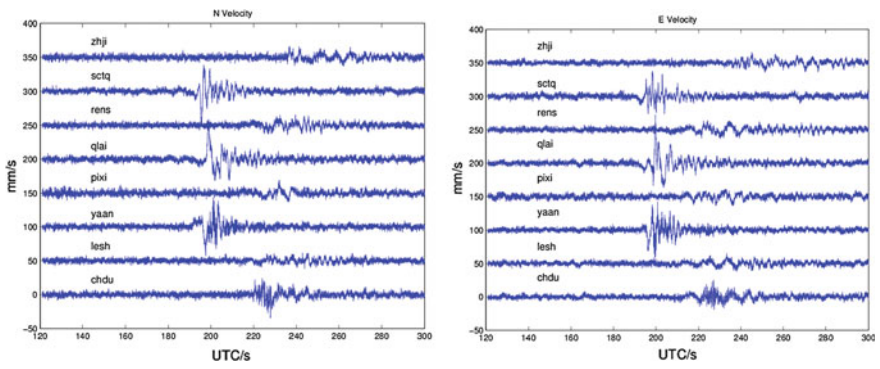**Fig. 8.2** The variety of site displacement during Lushan earthquake

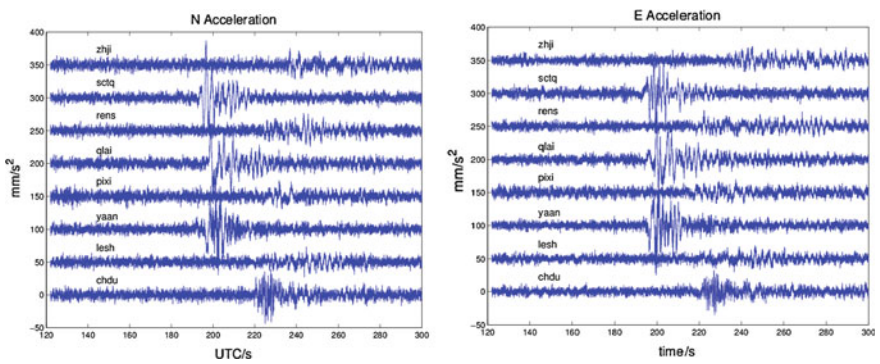**Fig. 8.3** The variety of site velocity during Lushan earthquake

Fig. 8.4 The variety of site acceleration during Lushan earthquake

Table 8.1 The impaction of site movement caused by earthquake

Site	Epicentral distance (km)	Peak amplitude (mm)		Peak velocity (mm/s)		Peak acceleration (mm/s^2)	
		N	E	N	E	N	E
CHDU	123	31.23	20.04	33.99	25.11	43.4	35.2
LESH	113	14.86	14.99	12.14	15	23.1	20.4
PIXI	112	15.99	14.87	18.33	13.79	24.5	19.9
QLAI	56	55.8	53.04	58.91	72.36	59	105.90
RENS	126	16.16	20.76	15.45	13.78	26.6	24.1
SCTQ	29	51.6	24.05	49.75	37.53	86.70	58.7
YAAN	21	42.38	48.72	43.64	42.18	69.8	82
ZHJI	195	19.07	15.66	16.43	15.58	25.2	20.5

series are not good, speared from 4–5 cm, we ignore the vertical displacements during Lushan Earthquake. The statistical table (Table 8.1) mainly shows the impaction of sites movement caused by earthquake. With carefully processed time series, the huge difference between different sites have been described below: the sites QLAI, SCTQ and YAAN nearby the epicenter are most activity, and peak displacement amplitudes of these sites have reached as high as 50 mm. Comparing to the rest sites, CHDU peak displacement amplitude on N direction is the biggest, which have reached 31 mm, and the peak accelerate has reached 105.9 mm/s^2, on E direction at QLAI site. However, GPS accelerate result would be quite smaller than accelerometer's result because of the ground resistance. While, comparing to displacement time series, the acceleration time series enlarge the impaction of earthquake, from which we can check the arriving time and lasting time of seismic wave more easily.

8.3 Analysis of Lushan Earthquake

8.3.1 Arriving Time of the P Wave

When the surface wave of a moderate-magnitude earthquake is treated as some kinds of energy from the model of point source, we can check it from the sites' acceleration time series. To check the arriving time of seismic wave (usually were treated as P wave), the method of S transform has been used. As a time–frequency distribution, S transform was developed in 1994 for analyzing geophysics data [10, 11]. In this way, the S transform is a generalization of the short-time Fourier transform (STFT), extending the continuous wavelet transform and overcoming some of its disadvantages. The improvement is the modulation sinusoids are fixed with respect to the time axis; this localizes the scalable Gaussian window dilations and translations in S transform. Moreover, the S transform doesn't have a cross-term

problem and yields a better signal clarity than Gabor transform. In our study, we used a fast S Transform algorithm invented by Brown in 2010. It reduces the computational time and resources by at least 4 orders of magnitude. The S transform function is showed as below:

$$S(\tau, f) = \int_{-\infty}^{\infty} h(t)w(\tau - t, f) \exp(-2\pi i f t) d\tau \tag{8.1}$$

$$\omega(\tau - t, f) = \frac{|f|}{\sqrt{2\pi}} \exp\left(\frac{-f^2(\tau - t)^2}{2}\right) \tag{8.2}$$

In the equation, the $h(t)$ represents the raw time series, $\omega(\tau - t, f)$ represents Gaussian window function, t, f, τ represent time, frequency, time scale factor using in the Gaussian window respectively.

In our experiment, we focus on the points at detect the energy of acceleration changing and the arriving time of P wave. The threshold value choosing is based on the method from document [11]. We find the result perform better by using S transform of these sites nearby Lushan epicenter comparing to the sites far away. That is mainly because when the epicentral distance is increased, the energy of P wave is getting less, which will cause the arriving time difficult to distinguish. We just list the figures of sites QLAI, SCTQ and YAAN, which have been showed from Figs. 8.5, 8.6 and 8.7. Since the arriving time of P wave at N direction and E direction is not the same, we employ a simple variable (horizontal displacement) which is defined as $dS = \sqrt{dN^2 + dE^2}$ to describe the movement characteristics, and the S transform has also been used at the acceleration of horizontal displacement to get the P wave arriving time. The first arrival time of seismic wave deriving from acceleration have been showed in Table 8.2.

From Table 8.2, we could find the P wave first arrive at YAAN site, the lag time for the seismic wave to CHDU is about 26 s. The differential time between YAAN and CHDU is very short but quite valuable. It can be definitely affirmed that the high rates GPS also have a huge potential usage in mainland early earthquake warning.

8.3.2 Rapid Epicenter Estimate

Crowell et al. [3] investigated the epicenter estimation only using the GPS data. They demonstrated that it is possible to estimate earthquake epicenter solely using GPS data. Utilizing high rates GPS to hypocenter location determination is a new approach which should be helpful. The classic method of determining hypocenter location attributes to Geiger and various linear methods based on it, such as the joint hypocenter determination, simultaneous structure and hypocenter determination,
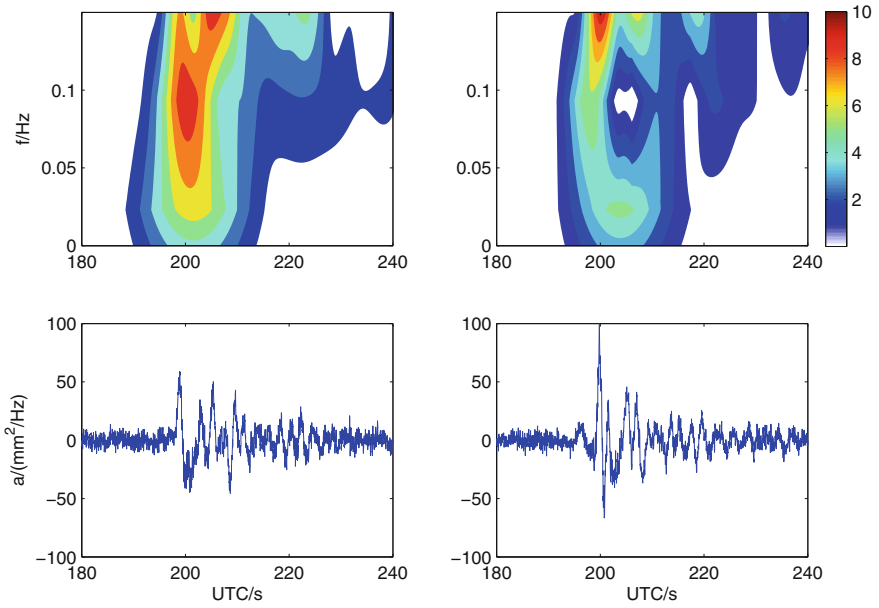
Fig. 8.5   The co-seismic frequency-domain on acceleration of QLAI site
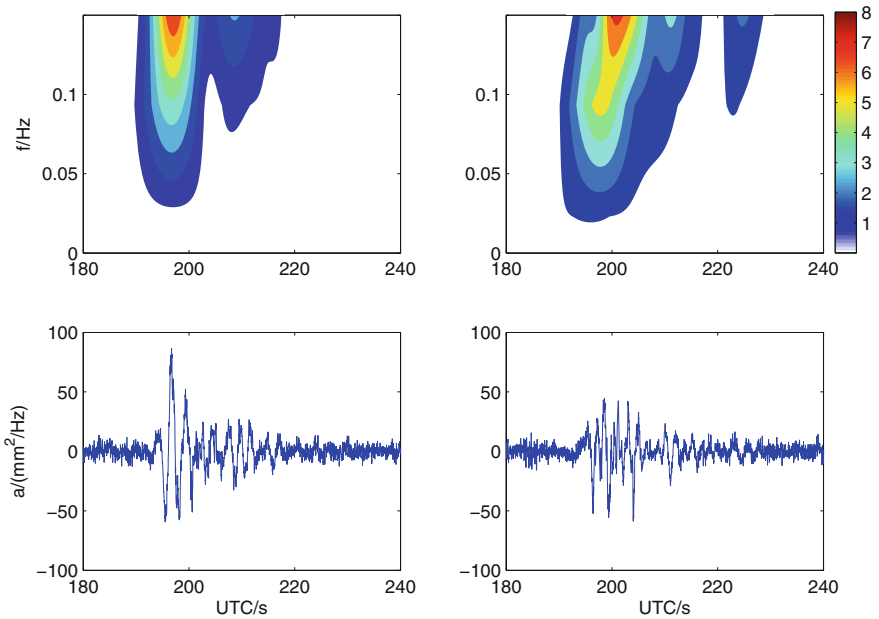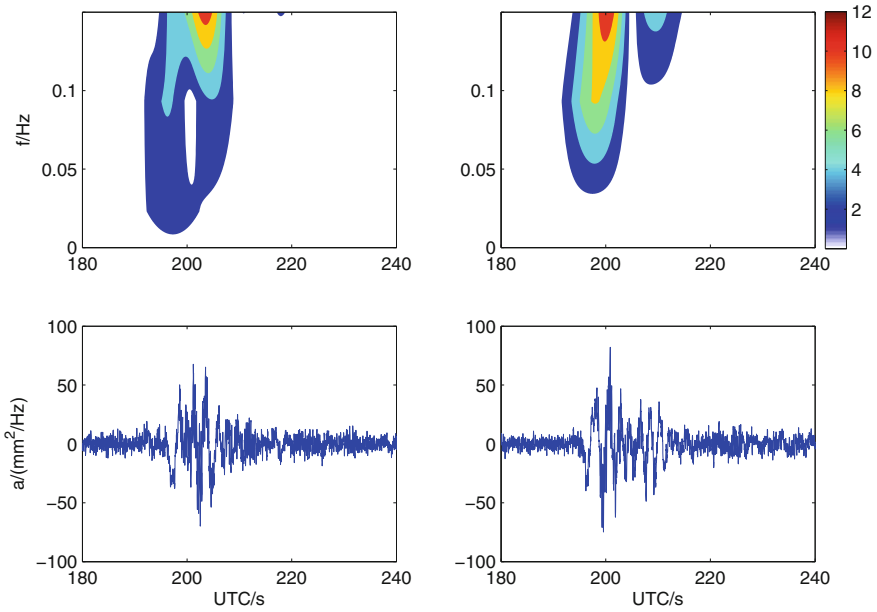

Fig. 8.6   The co-seismic frequency-domain on acceleration of SCTQ site

Fig. 8.7 The co-seismic frequency-domain on acceleration of YAAN site

Table 8.2 The arrival time of seismic wave deriving from acceleration

Sites	The offset time of acceleration (s)			
	N	E	Average	Horizontal displacement
CHDU	217.74	216.02	216.88	216.24
LESH	227.2	225.62	226.41	228.92
PIXI	226.76	223.46	225.11	228.34
QLAI	193.22	192.24	192.73	192.46
RENS	224.18	222.74	223.46	221.1
SCTQ	191.34	193.28	192.31	191.7
YAAN	190.98	190.52	190.75	190.8
ZHJI	233.32	234.94	234.13	235.4

relative location technique, and double-difference location algorithm. By using the classic approach state above, at least four well geographic distribution sites' location coordinates are needed to invert the accurate hypocenter location. While, in our study, in order to determine the hypocenter fast and precisely, we use a geometry approach of searching in three-dimension to check the appropriate point source. An equation which using a least-squares fitting algorithm to invert the hypocenter location and the seismic event start time have been established as below:

$$f(T_0, N_0, E_0, U_0) = \min \sum_{i=1}^{n} d_i^2 \qquad (8.3)$$

$$d_i = \sqrt{(N_i - N_0)^2 + (E_i - U_0)^2 + (U_i - U_0)^2} - v(t_i - T_0) \qquad (8.4)$$

where t_i is the seismic P wave arrival time at site i, N_i, E_i, U_i is the coordinate of site i, T_0, N_0, E_0, U_0 represent the seismic event trigger time and the coordinate in NEU components respectively.

Once three sites have detected the seismic wave, the equation would have a unique solution which can be treated as the initial point source location and seismic event time. However, as the epicentral distance increased, the weight factors of the other sites shall be down because of the uncertainty of P wave velocity. Here, for quasi real-time determine the hypocenter location position, we invert the initial seismic location position and nuclear time just by using three sites at which P wave is first arriving. Since YAAN site have first detected the P wave, we take it as the origin center point. A range of 2° on latitude and longitude out of the center point, and 30 km depth has been chosen. To search for the optimal hypocenter location, we take Eq. (8.3) as the judgment rule. The search steps of horizontal direction is set at 1°, 0.5°, 0.1°, 0.01° respectively, and the depth step is set at 5, 1, 0.5, 0.1 km respectively. After the optimal grid searching, an appropriate location position has been determined as the position of (30.04N, 103.05E), at the depth of 16.7 km, and the initial seismic event time as GPS Time 183.71 s. If added 16 leap seconds from 1982, covert to Beijing time it is 8:02:47.71. The seismic P wave velocity is about 7.11 km/s to YAAN site, 7.02 km/s to SCTQ site, and 7.01 km/s to QLAI site respectively. Therefore, the average spread speed is 7.05 km/s, quite confirms to the seismic P wave's characteristics. The spread time to the three sites is 4.11, 6.71 and 9.05 s respectively.

8.3.3 Magnitude Inversion

As high rate GPS data can provider with a high signal-to-noise ratio (SNR) and precisely determine the peak horizontal displacement, but not sensitive to the P wave. We just investigate the surface wave magnitude derived by GPS. A general form for surface wave magnitude scales can be defined as [8]:

$$M = \log(A/T) + a \log(\Delta) + b \qquad (8.5)$$

where A is the peak displacement (including the N E U component) caused by the seismic waves, T is the dominant period of the measured waves, a is the coefficient correction for epicentral distance, and b is a constant. The logarithmic scale is usually used because the seismic wave amplitudes of earthquakes vary enormously.

Fig. 8.8 Relationship
between peak horizontal
displacements and epicentral
distance
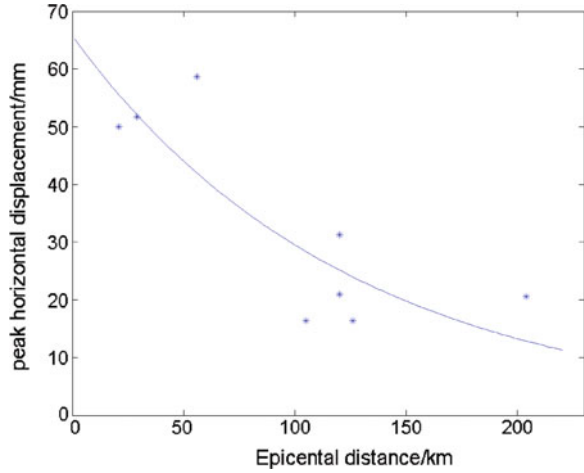
Table 8.3 Magnitude statistic of sites derived from the surface wave

Sites	Peak displacements (mm)	Epicentral distance (degree)	Magnitude
CHDU	31.17	0.98	6.48
PIXI	27.41	0.89	6.36
QLAI	57.69	0.27	5.82
RENS	21.31	0.96	6.30
SCTQ	51.16	0.30	5.85
YAAN	49.31	0.32	5.87
ZHJI	21.13	1.51	6.62
Regression			6.18

Recent studies have shown that the displacement waveforms derived from high-rate GPS data are consistent with those measured by strong-motion records [2, 13]. Thus, no matter if the displacement waveforms are measured by a seismometer or by GPS, the empirical relation-ship Eq. (8.5) is appropriate for magnitude estimates based on far-field surface waves. Gutenberg (1945) deduced an empirical relationship between peak displacement, distance and magnitude by utilizing the strong-motion [7]. He used an empirical regression method to resolve the coefficient correction a and constant b by the amplitude of surface waves from a set of earthquakes that occurred in California, namely

$$M = \log(A) + 1.66 \log(\Delta) + 2.0, \tag{8.6}$$

Here, which is different from Eq. (8.5), A is the peak horizontal displacement derived from surface waves in units of micrometer, Δ is the epicentral distance in units of degree. M is the magnitude. We use the empirical relationship to build a magnitude evaluate figure, as shown in Fig. 8.8 (Table 8.3).

8.4 Conclusion Remarks

Study shows that 50 Hz GPS measurements have the potential usage on seismic relief, the epicenter, trigger time can be determined quickly about 60 s. Magnitude size also could be determined within nearly 300 s. The searching result of epicenter location is quite close to USGS' results (as shown in Fig. 8.1), and the seismic event start time is 1.71 s less. While, the magnitude determining is different from the announce result of China Seismological Bureau. Especially when the epicentral distance is below $0.5°$, the magnitude size estimate is lower apparently. We consider that it may be caused by the assuming empirical equation developed by Gutenberg is not quite suitable in Sichuan, China, from which we consider the GPS observation shall be built at a new equation for magnitude determine.

Dense VHRGPS networks will be very helpful to detect significant variations in the seismic wave propagation, that could be related to rupture dynamics or otherwise hidden geologic heterogeneities and as an earthquake magnitude is bigger, the outcome will be better observed. We find although the seismic wave first arrive YAAN site, the site coordinate time series which impacted most intensity is QLAI site. The phenomena could relate to the hidden geologic heterogeneities.

References

1. Avallone A, Marzario M, Cirella A, Piatanesi A, Rovelli A, Di Alessandro C, D'Anastasio E, D'Agostino N, Giuliani R, Mattone M (2011) Very high rate (10 Hz) GPS seismology for moderate-magnitude earthquakes: the case of the Mw 6.3 L'Aquila (central Italy) event. J Geophys Res Solid Earth 116:B2305
2. Bock Y, Crowell BW, Kedar S, Melgar Moctezuma D, Squibb MB, Webb F, Yu E, Clayton RW (2010) Observations and modeling of the Mw 7.2 2010 El Mayor-Cucapah Earthquake with real-time high-rate GPS and accelerometer data: implications for earthquake early warning and rapid response, vol 1, p 5
3. Crowell BW, Bock Y, Squibb MB (2009) Demonstration of earthquake early warning using total displacement waveforms from real-time GPS networks. Seismol Res Lett 80:772–782
4. Delouis B, Nocquet J, Vallée M (2010) Slip distribution of the February 27, 2010 Mw = 8.8 Maule Earthquake, central Chile, from static and high-rate GPS, InSAR, and broadband teleseismic data. Geophys Res Lett 37:L17305
5. Larson KM (2009) GPS seismology. J Geodesy 83:227–233
6. Larson KM, Bilich A, Axelrad P (2007) Improving the precision of high-rate GPS. J Geophys Res Solid Earth (1978–2012) 112
7. Gutenberg B (1945) Amplitudes of surface waves and magnitudes of shallow earthquakes. Bulletin of the eismological Society of America, 35(1): 3-12

8. Richter CF (1935) An instrumental earthquake magnitude scale. Bull Seism Soc Am 25:1–32
9. Shi C, Lou Y, Zhang H, Zhao Q, Geng J, Wang R, Fang R, Liu J (2010) Seismic deformation of the Mw 8.0 Wenchuan earthquake from high-rate GPS observations. Adv Space Res 46:228–235
10. Stockwell RG (2007) Why use the S-transform. AMS Pseudo Differ Operators Partial Differ Eqn Time Freq Anal 52:279–309
11. Stockwell RG, Mansinha L, Lowe RP (1996) Localisation of the complex spectrum: the S transform. J Assoc Explor Geophysicists 17:99–114
12. Yin H, Wdowinski S, Liu X, Gan W, Huang B, Xiao G, Liang S (2013) Strong ground motion recorded by high-rate GPS of the 2008 Ms 8.0 Wenchuan Earthquake, China. Seismol Res Lett 84:210–218
13. Zheng Y, Li J, Xie Z, Ritzwoller MH (2012) 5 Hz GPS seismology of the El Mayor-Cucapah earthquake: estimating the earthquake focal mechanism. Geophys J Int 190:1723–1732